Volume 1 | Number 1 | Jan 2013 | Pages 1–100

Dalton Transactions

An international journal of inorganic chemistry
www.rsc.org/dalton

ROYAL SOCIETY OF CHEMISTRY

This is an *Accepted Manuscript*, which has been through the Royal Society of Chemistry peer review process and has been accepted for publication.

Accepted Manuscripts are published online shortly after acceptance, before technical editing, formatting and proof reading. Using this free service, authors can make their results available to the community, in citable form, before we publish the edited article. We will replace this *Accepted Manuscript* with the edited and formatted *Advance Article* as soon as it is available.

You can find more information about *Accepted Manuscripts* in the **Information for Authors**.

Please note that technical editing may introduce minor changes to the text and/or graphics, which may alter content. The journal's standard **Terms & Conditions** and the **Ethical guidelines** still apply. In no event shall the Royal Society of Chemistry be held responsible for any errors or omissions in this *Accepted Manuscript* or any consequences arising from the use of any information it contains.

Journal Name

ARTICLE

Challenges in assignment of orbital populations in a high spin manganese(III) complex

A. J. Fitzpatrick[a], S. Stepanovic,[b] H. Müller-Bunz,[a] M. A. Gruden-Pavlović,[b] P. García-Fernández,[c] and G. G. Morgan[a]*

Magnetic, structural and computational data of four complex salts with the same mononuclear high spin octahedral Mn(III) complex cation are reported. The manifestation of Jahn-Teller-like distortions in the Mn(III) cation is dependent on the nature of the charge-balancing anion, with small anions yielding a planar elongation and large anions freezing out a preferential axial elongation along one of the amine-Mn-imine directions within that same plane. Modulation of the lattice by changing the charge balancing anion results in mixing of the orbital symmetry due to vibrational perturbation.

Introduction

Jahn–Teller effects are fundamentally dynamic in nature: in the idealised case the distortion is fluxional and oscillates between a number of degenerate states.[1] In this case the only energetic consideration that could impose a barrier is the energy required to change between conformations. Dynamic Jahn-Teller effects have been studied extensively in solid state perovskite manganites. Here it was recognised that the orbital degree of freedom plays an important role in many magnetic and electronic properties and that temperature dependent orbital ordering transitions can be observed.[2-4] However in reality, a static distortion is usually observed, *i.e.* one direction is preferred due to the constraints of the local environment (*e.g.* defects or crystal packing), and this is most commonly manifest as a tetragonal elongation along the z-axis.[5] In transition metal chemistry the effect has been studied most intensively in Cu(II)[6-11] and Mn(III) complexes.[12-18] An alternative, and much less common, manifestation of the distortion is equatorial expansion, commonly termed axial compression, which is typically ascribed to preferential population of the $d_{x^2-y^2}$ orbital rather than d_{z^2}. Several examples of axial compression in Mn(III)[19-21] and Cu(II)[22-27] have been published, including several examples of what was first thought to be a compression but which later turned out to be a dynamic axial elongation in Cu(II).[22-27] Use of the the term "axial compression" can be misleading as (i) in systems with different axial and equatorial ligands (or intrinsic low-symmetry) the metal-ligand distances along axis and equatorial plane will naturally be different due to the differences in bonding, an effect unrelated to a proper Jahn-Teller effect; (ii) in these cases, vibronic phenomena like the pseudo Jahn-Teller effect, may further lower the symmetry simultaneously increasing (lowering) the distance with two equatorial ligands yielding an elongation in a non-axial direction rather than a compression.[28, 29] These are all important factors when analysing apparent "axial compressions" in Mn(III). Thus, while many of these systems do not display a true Jahn-Teller effect many interesting phenomena, such as further symmetry-lowering distortions or orbital ordering, that closely resemble the Jahn-Teller effect, appear in these systems. Here we will denote these effects and distortions as Jahn-Teller-like to distinguish them from a true Jahn-Teller effect.[28, 29]

Octahedral Mn(III) complexes also have an extra degree of spin

[Mn(taa)]   [Mn(R-Sal₂323)]⁺   [Mn(R-Salk₂323)]⁺
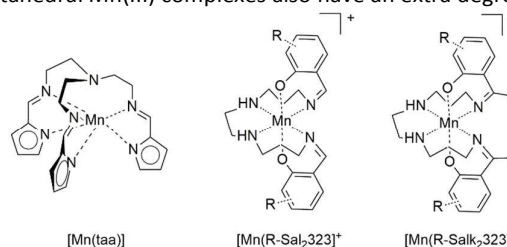
freedom compared with Cu(II) in that there exists more than one possible spin state. Three spin arrangements could exist in theory for a d^4 ion: fully spin paired (S=0), fully unpaired (S=2) or one paired set and two unpaired (S=1). In reality only S=1 and S=2 spin states have been observed in small molecule complexes and a small subset of these show thermal switching between the high spin (HS) S=2 and the so-called low spin (LS) S=1 states.[30-41] As both the S = 1 and S = 2 states are Jahn-Teller active it is of interest to examine how the distortion is manifest in the HS form of spin crossover (SCO) complexes

a School of Chemistry, University College Dublin, Belfield, Dublin 4, Ireland
b Faculty of Chemistry, University of Belgrade, Studentski trg 12-16, 11000 Beograd, Republic of Serbia
c Departamento de Ciencias de la Tierra y Física de la Materia Condensada, Universidad de Cantabria, 39005 Santander, Spain.
 Email: grace.morgan@ucd.ie

after thermal switching from the S = 1 ground state. The majority of published reports on d^4 SCO have been on salts of [Mn(R-Sal$_2$323)]$^+$ cations, where R-Sal$_2$323 is a hexadentate dianionic Schiff base ligand.[28,30-33,38] To date an axial compression has been suggested for the HS forms of such complexes which has prompted some computational studies[40, 41] with the starting assumption that the magnetic orbital is $d_{x^2-y^2}$.

However the earliest SCO Mn(III) example, the neutral [Mn(taa)] complex,[30] has been the subject of many more computational and experimental studies[42-46] than complexes of the [Mn(R-Sal$_2$323)]$^+$ series, and in particular, variable temperature Raman and dielectric measurements suggest population of d_z^2 and a dynamic Jahn-Teller effect in the HS state.[47] Nakano *et al*. report that their Raman data and computational studies indicate a lower vibrational contribution to the transition entropy than is typical for iron SCO complexes. Although this point has been disputed by Garcia *et al*.,[48] the discovery of an electronic dynamic disorder in the HS phase by dielectric measurements provided an alternative entropy source to explain the thermally-induced SCO transition. This dynamic disorder was attributed to the reorientation of the dipoles accompanying the $E \otimes e$ Jahn-Teller effect in the HS manganese(III) ions *i.e.* ferroelectric ordering.[47]

We were therefore motivated to further investigate the nature of the Jahn-Teller-like distortion in HS complexes of Mn(III) with R-Sal$_2$323 type ligands. Population of the $d_{x^2-y^2}$ orbital was first proposed by us as an explanation for the significant elongation (0.1 Å) of all four Mn-N distances on switching from LS to HS with no accompanying change to the Mn-O oxygen bond lengths.[31] Here we report structural studies on four salts of a new mononuclear Mn(III) complex cation, [Mn(5F-Salk$_2$-323)]$^+$, which call into question the earlier assignment of orbital populations in related HS [Mn(R-Sal$_2$323)]$^+$ complexes. The original R-Sal$_2$323 ligand design was modified in the present study with replacement of the imine bonds with ketimines so as to investigate the effect of ligand constraint on Mn(III) spin state. This was pursued with the expectation that spin crossover would be curtailed or forced to follow an abrupt pathway. The outcome was that the S=2 HS state was stabilized in all isolated salts of [Mn(5F-Salk2-323)]$^+$ suggesting that a more flexible ligand framework is essential for spin state switching with this donor set.

Results and Discussion

Assembly of [Mn(5F-Salk$_2$-323)]$^+$ was readily achieved in ethanol/acetonitrile solution, Scheme 1, and four different salts, (**1**)-(**4**), were isolated as dark brown crystals by addition of ammonium, sodium or silver salts of the appropriate anion and standing overnight. Elemental analysis and mass spectrometry confirmed the formation of [Mn(5F-Salk$_2$-323)]CF$_3$SO$_3$, (**1**), [Mn(5F-Salk$_2$-323)]PF$_6$, (**2**), [Mn(5F-Salk$_2$-323)]SbF$_6$, (**3**) and [Mn(5F-Salk$_2$-323)]BPh$_4$, (**4**).

Scheme 1: Synthesis of [Mn(5F-Salk$_2$-323)]X complexes (**1**)-(**4**).

X =
1 = CF$_3$SO$_3$
2 = PF$_6$
3 = SbF$_6$
4 = BPh$_4$
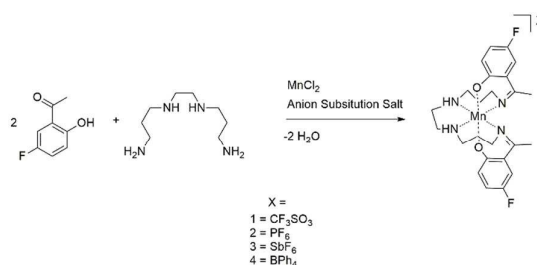
Magnetic Characterisation

Variable temperature magnetic susceptibility data for pol-crystalline samples of (**1**)-(**4**) was recorded on a Quantum Design MPMS® XL-7 SQUID magnetometer in a field of 0.5 T between 10 – 300K in heating and cooling modes for (**1**) and (**3**), and between 300 K and 20 K for (**2**) and (**4**). The plots of $\chi_M T$ vs. temperature for (**1**) – (**4**) are shown in Fig. 1. The constrained ligand stabilised the high spin state in all cases as the $\chi_M T$ value is close to the spin only value of 3 cm^3 mol^{-1} K expected for an S=2 ion. The drop in the $\chi_M T$ value in the low temperature regime is the result of significant zero field splitting due to the anisotropic nature of the Mn(III) ion in an octahedral field. The use of a more sterically constrained di-ketimine ligand in place of a di-imine switches off the ability to promote SCO in this series.
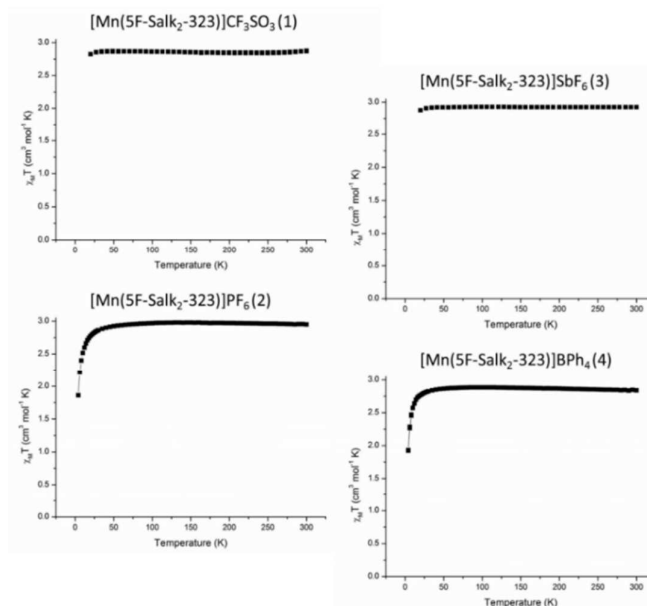

Fig. 1: χ_MT v. T plots for complexes (**1**)-(**4**) between 10-300 K indicating an S= 2 spin state.

Structural Characterisation

Single crystal X-ray diffraction at 100 K was used to characterise the solid state structure of complexes (**1**)-(**4**). Two aspects were studied in particular: (i) bond length data in the immediate coordination sphere of the [Mn(5F-Salk$_2$-323)]$^+$ cation to investigate the orbital population associated with the Jahn-Teller-like distortion, and (ii) local distortion from octahedral geometry, which should be higher if the distortion is frozen out rather than averaged. All complexes crystallised

Journal Name ARTICLE

in monoclinic space groups, isostructural complexes (**1**) and (**2**) in P2$_1$/n, (**3**) in C2/c and (**4**) in P2$_1$/c. The crystallographic data for each is listed in Table 1 with bond length data in Table 2.

The asymmetric units of complexes (**1**), (**2**) and (**4**) comprise one full occupancy cation and one full occupancy anion. The

asymmetric unit of complex (**3**) consists of one full occupancy cation and two half occupancy hexafluoroantimonate anions. In all cases geometry around the central manganese ion is *pseudo*-octahedral with *trans*-oxygen and pairs of *cis*-amine and *cis*-imine nitrogen donors, Figure 2.

Table 1: Crystallographic data for complexes 1-4.

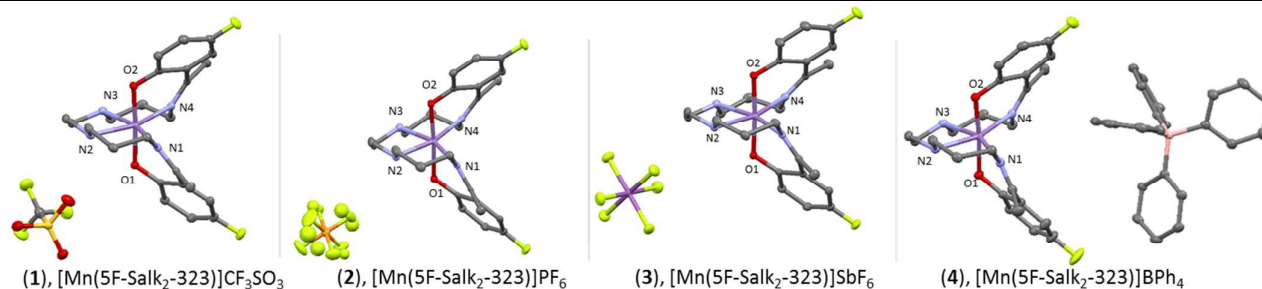| Complex Number	(**1**) [Mn(5F-Salk$_2$-323)]CF$_3$SO$_3$	(**2**) [Mn(5F-Salk$_2$-323)]PF$_6$	(**3**) [Mn(5F-Salk$_2$-323)]SbF$_6$	(**4**) [Mn(5F-Salk$_2$-323)]BPh$_4$
Empirical formula	C$_{25}$ H$_{30}$ N$_4$ O$_5$ F$_5$ S Mn	C$_{24}$ H$_{30}$ N$_4$ O$_2$ F$_8$ P Mn	C$_{24}$ H$_{30}$ N$_4$ O$_2$ F$_8$ Mn Sb	C$_{48}$ H$_{50}$ B N$_4$ O$_2$ F$_2$ Mn
Formula weight	648.53	644.43	735.21	818.67
Crystal system	Monoclinic	Monoclinic	Monoclinic	Monoclinic
Space group	P2$_1$/n	P2$_1$/n	C2/c	P2$_1$/c
Z	4	4	8	4
a(Å)	10.9926(2)	10.5207(3)	26.4731(3)	12.1375(1)
b(Å)	17.3651(3)	17.2468(4)	10.7771(1)	17.1630(1)
c(Å)	14.5485(2)	14.5757(3)	19.8816(2)	19.5734(2)
α(deg)	90	90	90	90
β(deg)	97.061(1)	95.459	109.193(1)	97.0378(8)
γ(deg)	90	90	90	90
V(Å^3)	2756.07(8)	2632.74(11)	5357.00(10)	4046.73(6)
P(calc) Mg/m3	1.563	1.626	1.823	1.344
μ(mm^{-1})	0.632	0.650	1.567	0.381
R$_1$(I >2σ(I))	0.0316	0.0437	0.0188	0.0355
wR$_2$ (all data)	0.0778	0.1129	0.0472	0.0914

(**1**), [Mn(5F-Salk$_2$-323)]CF$_3$SO$_3$ (**2**), [Mn(5F-Salk$_2$-323)]PF$_6$ (**3**), [Mn(5F-Salk$_2$-323)]SbF$_6$ (**4**), [Mn(5F-Salk$_2$-323)]BPh$_4$

Fig. 2: Structures of complexes (**1**)-(**4**) at 100 K. Ellipsoids at 50% probability.

Table 2: Experimental bond lengths for complexes (**1**)-(**4**) and calculated bond lengths for the [Mn(5F-Salk2-323)]$^+$ cation (final column). * = Distorted axes for (**3**) and (**4**).

	Bond Lengths (Å)				
	(**1**) CF$_3$SO$_3$	(**2**) PF$_6$	(**3**) SbF$_6$	**4** BPh$_4$	**Theory**
Mn-O1$_{phen}$	1.8697(10)	1.8621(17)	1.8652(8)	1.8610(9)	1.8833
Mn- O2$_{phen}$	1.8594(10)	1.8555(17)	1.8650(7)	1.8764(9)	1.8826
Mn-N1$_{im}$	2.1192(12)	2.162(2)	2.1087(9)	2.1702(11)*	2.1211
Mn-N4$_{im}$	2.1551(12)	2.103(2)	2.1399(9)*	2.1040(11)	2.1296
Mn-N2$_{am}$	2.2162(13)	2.232(2)	2.2620(10)*	2.1840(11)	2.3490
Mn-N3$_{am}$	2.2328(13)	2.230(2)	2.1994(9)	2.3050(11)*	2.3410

At first glance the long Mn-N distances in all four structures suggest population of the d$_{x^2-y^2}$ orbital in the [Mn(5F-Salk$_2$-

323)]$^+$ cation, but the disparity between the pairs of trans N$_{am}$-Mn-N$_{im}$ distances in complexes (**3**) and (**4**) argues against this simple interpretation. The O1–Mn–O2 distance does not vary significantly across the four complexes so it can be concluded that the orbital population, whether in d$_z^2$-like or d$_{x^2-y}$-like orbitals, lies within the N4 plane around the Mn. In the BPh$_4$$^-$ complex, (**4**), the N1$_{im}$-Mn-N3$_{am}$ distance of 4.48 Å is 0.2 Å longer than the corresponding N4$_{im}$-Mn-N2$_{am}$ axis of 4.28 Å, Table 2, suggesting that the Jahn-Teller-like distortion is manifest as an axial elongation along N1$_{im}$-Mn-N3$_{am}$. A similar elongation is observed in the SbF$_6$$^-$ salt, with one N$_{im}$-Mn-N$_{am}$ axis significantly longer than the other, although in this case the difference is less pronounced: N4$_{im}$-Mn-N2$_{am}$ (4.40 Å) is 0.1 Å longer than N1$_{im}$-Mn-N3$_{am}$ (4.31 Å), Table 2. At 100 K there is no significant difference between the pairs of N$_{im}$-Mn-N$_{am}$ axes within the remaining two complexes [Mn(5F-Salk$_2$-323)]CF$_3$SO$_3$, (**1**) and [Mn(5F-Salk$_2$-323)]PF$_6$, (**2**). In both cases one Mn-N$_{im}$ distance is slightly longer than the other but the N$_{am}$-Mn-N$_{im}$ distance averages to *circa* 4.3 Å in both complexes suggesting a symmetric distortion for the[Mn(5F-Salk$_2$-323)]$^+$ cation in the lattices with the smaller CF$_3$SO$_3$$^-$ and PF$_6$$^-$ lattices, Figure 4.
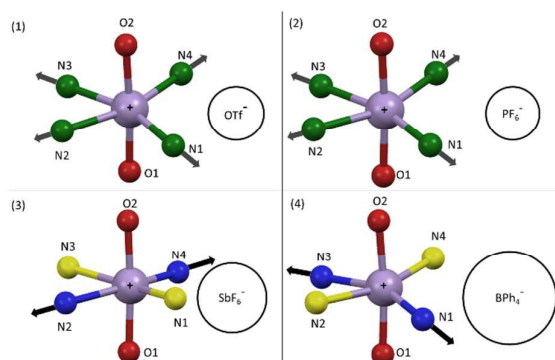

Fig. 4: Coordination spheres for the [Mn(5F-Salk2-323)]$^+$ cation with different anions highlighting the nature of the Jahn-Teller-like distortion. In complexes (**1**) and (**2**) the distortion is pseudo-symmetric in the N4 plane. In complexes (**3**) and (**4**) the distortion freezes out in one direction with preferential axial elongation in one direction. In (**3**) elongation is along N2-Mn-N4 (blue) with shortening of the N1-Mn-N3 axis (yellow), in complex (**4**) this pattern is reversed.

The pronounced equatorial elongation in the BPh$_4$$^-$ complex (**4**) is also reflected in the large distortion parameters of this salt compared with the CF$_3$SO$_3$$^-$, PF$_6$$^-$ and SbF$_6$$^-$ analogues, Table 3. We have recently compared Σ and θ distortion parameters for two series of [Mn(R-Sal$_2$323)]$^+$ complexes in both LS and HS structural forms which revealed a larger change in the trigonal distortion θ compared to the overall deviation from 90° angles (Σ).[36] Typical distortion values for HS and LS Mn(III) are generally lower than for Fe(II)[49] or Fe(III),[50] Table 3, which is expected given that the HS form of Mn(III) will experience a Jahn-Teller-like distortion which will predominantly affect bond lengths, but may assist conservation of more regular angles compared with Fe(II) or Fe(III).

Table 3: Distortion parameters of complexes 1-4 and ranges for Mn(III),[33] Fe(III)[47] and Fe(II).[46]

Complex	(1)	(2)	(3)	(4)
θ/°	151.58	159.07	160.46	186.52
Σ/°	62.5	65.19	60.15	82.02
		LS	HS	
θ/°	Mn(III)	80 - 100	140 - 220	
Σ/°		30 - 46	60 - 70	
θ/°	Fe(III)	56 - 98	204 - 358	
Σ/°		40 - 47	86 - 118	
θ/°	Fe(II)	270 - 316	450 - 500	
Σ/°		70-80	150-200	

The Σ and θ parameters of complexes (**1**)-(**3**) are in line with those of the previously reported HS Mn(III) complexes[36] with Σ values between 60-65° and θ values of 150-160°. Those for the BPh$_4$$^-$ complex (**4**) are, however, significantly larger with Σ = 82° and θ = 187°, which is to be expected given the anisotropic nature of the distortion along one axis.

It is surprising that the nature of the distortion changes so markedly within one complex cation when it is embedded in different lattices, *i.e.* with different anions. Packing interactions were therefore examined in order to investigate the effects of hydrogen bonding or other types of connectivity in driving a asymmetric or symmetric Jahn-Teller-like distortions. Three packing motifs emerged from examination of the four structures: halogen bonded dimers for (**1**) and (**2**); a halogen bonded 1-D chain for complex (**3**) and discrete non-interacting cations and anions in complex (**4**). In the case of complexes (**1**) and (**2**) pairs of cations are linked by halogen-π$_{aryl}$ interactions between peripheral ligand fluorine atoms and the phenyl rings of the nearest neighbour, shown for complex (**1**) in Figure 5.
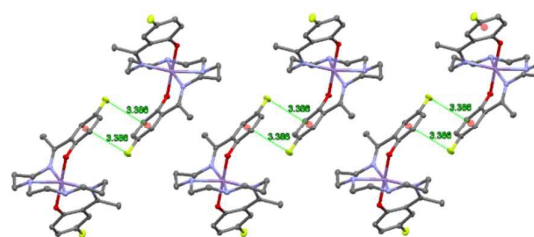

Fig. 5: F- π$_{aryl}$ bonding dimer arrangement in complex (**1**).

There is also hydrogen bonding between the amine hydrogen and the oxygen of the triflate anion in complex (**1**) which forms a 1-D H-bonding chain, Figure S1, which is not present in complex (**2**), Figure S2.

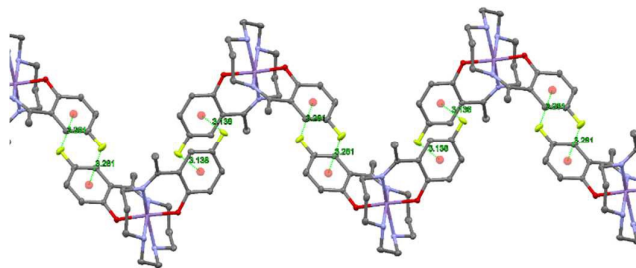In (**3**) the same type of F-π$_{aryl}$ interaction links adjacent complex cations into a 1-D chain, Figure 6.

Fig. 6: Zig-zag F- π_{aryl} bonding 1-D chain in complex (**3**).

The F-π_{aryl} distances of 3.38 Å. 3.19 Å and 3.28 Å, for complexes (**1**), (**2**) and (**3**), respectively are all within the published range for such interactions.[51-53] In contrast to the high level of connectivity in complexes (**1**)-(**3**), the [Mn(5F-Salk$_2$-323)]$^+$ cations in complex (**4**) are well insulated with no obvious intermolecular interactions. Instead each cation is surrounded by channels of BPh$_4$$^-$ anions, thereby hindering any halogen interactions between adjacent complex cations, Figure 7.
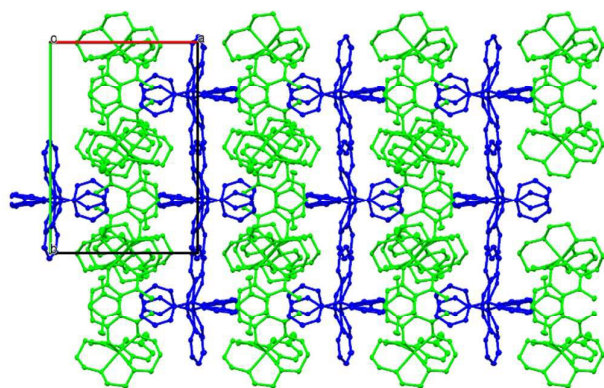

Fig. 7: Packing diagram of complex (**4**), displaying the channels of cation and anions. Cation in green and anion in blue.

It therefore appears that where there is good connectivity between adjacent transition metal cations the distortion is symmetric, however once the cations are isolated in the lattice by using a large anion, the Jahn-Teller-like distortion freezes out in one direction, causing an asymmetric distortion in the preferential ordering of the immediate coordination sphere along one set of N$_{im}$-Mn-N$_{am}$ donors sets. This highlights the dynamic nature of the distortion

Computational Studies

To further investigate the electronic properties of these complexes, DFT calculations were performed using the BP86 generalized gradient approximation (GGA) functional and the hybrid B3LYP, resulting in comparable results. The orbitals in these simulations were represented with standard Slater-type

triple-zeta plus polarization (TZP) basis set included with the code. Geometries were relaxed under a stringent geometry cutoff (0.0001) due to the softness of some vibrational modes that produced significant variations of the final geometry under less restrictive conditions. Calculations for the HS configuration of the isolated Mn(III) cation without counter anion *in vacuo* resulted in (i) an electronic ground structure where the HOMO corresponds to an x^2-y^2-like orbital and the LUMO a $3z^2$-r^2-like orbital, Figs S5 and S6, (ii) metal-ligand distances, associated with the strong manganese oxygen bond, close to 1.88 Å in good agreement with experimental values and (iii) two-asymmetric equatorial trans N-Mn-N bonds whose average Mn-N distance is the same and close to 2.23Å. These equatorial geometries do not correlate well to the experimental bond lengths, Table 2, particularly in the case of complex 4 where there is a calculated symmetric stretch which in reality is the most pronounced example of a preferential elongation in the Mn-N donors. This serves to show that the equatorial bonds are much softer than the axial ones and are, in fact, quite sensitive to perturbations such as the identity of the counterion used to grow the various crystals.

In must be stressed here that vibronic effects, like the *pseudo* Jahn-Teller effect are very sensitive to the intrinsic softness of the distortion mode, usually denoted by the force constant K_0 and the separation between the two coupled electronic states.[54] The instability condition is the point where the vibronic effects fully compensate K_0 yielding a null force constant in the ground state. In our particular case, when the vibrational frequencies of the complex were obtained at the relaxed geometry, b_1-like vibrations were identified with low frequency (see Fig. S7) which drive the elongation along one equatorial axis with compression along the other. This is consistent with a pseudo Jahn-Teller model associated with HOMO-LUMO mixing. Calculations of the energy profile along this distortion (not shown) result in an extremely flat energy landscape that could easily be perturbed by the presence of a large anion.[51] This gives credence to the change observed experimentally when a change in anion size is the major variable among the four complexes. If the triggering of the mixing of HOMO-LUMO states by anion size results in atypical manifestations of the JT distortion, it explains the discrepancy between the experimentally observed bond lengths and the computationally calculated *in vacuo* cation only bond lengths.

Conclusions

Here the effects of ligand constraint and crystal packing on choice of spin state and the nature of the Jahn-Teller-like distortion in a mononuclear Mn(III) Schiff base complex were investigated. Use of a constrained di-ketimine ligand was found to stabilise HS Mn(III) in contrast to complexes with related di-imine ligands which promoted SCO. This highlights the structural flexibility necessary for promoting thermal spin transitions in Mn(III) with this ligand set. The nature of the distortion in the complex cation was also investigated in four different crystalline lattices with different anions in tandem with DFT calculations of the *in vacuo* complex cation which

assumed population of the $d_{x^2-y^2}$ orbital. The discrepancy between experimental and calculated bond lengths point towards a non-trivial electronic structure. Our structural and computational studies indicate the appearance of a mixed-orbital ground state with both equatorial and axial character depending on the counterion employed. This is mainly due to the presence of low symmetry and therefore a true Jahn-Teller effect cannot be invoked as a good description. The situation rather resembles a pseudo-Jahn-Teller effect (PJTE) close to the instability where concomitant distortion and mixture of orbitals is susceptible to perturbation by outside influences such as anion size. This opens up avenues for future investigation on PJTE in low symmetry complexes with ligands such as R-Sal$_2$323 and its analogues.

Acknowledgements

Notes and references

Structures of **1** (CCDC no. 1417930), **2** (CCDC no. 141791), **3** (CCDC no. 1417932) and **4** (CCDC no. 1417929) deposited at the Cambridge Crystallographic Data Centre.

1.   L. R. Falvello, *J. Chem. Soc., Dalton Trans.*, 1997, 4463-4476.
2.   I. K. Kliment and D. I. Khomskiĭ, *Phys. Up.*, 1982, **25**, 231.
3.   C. N. R. Rao, *J. Phys. Chem. B*, 2000, **104**, 5877-5889.
4.   Y. Tokura and N. Nagaosa, *Science*, 2000, **288**, 462-468.
5.   P. García-Fernández, A. Trueba, M. T. Barriuso, J. A. Aramburu and M. Moreno, in *Vibronic Interactions and the Jahn-Teller Effect: Theory and Applications, Progress in Theoretical Chemistry and Physics*, 2012, **23** 105-142, Eds. M. Atanasov, C. Daul and P. Tregenna-Piggott.
6.   J. Gazo, I. B. Bersuker, J. Garaj, M. Kabesova, J. Kohout, H. Langfelderova, M. Melnik, M. Serator and F. Valach, *Coord. Chem. Rev.*, 1976, **19**, 253-297.
7.   S. Alvarez, M. Julve and M. Verdaguer, *Inorg. Chem.*, 1990, **29**, 4500-4507.
8.   M. D. Towler, R. Dovesi and V. R. Saunders, *Phys. Rev. B: Condens. Matter*, 1995, **52**, 10150-10159.
9.   I. Persson, P. Persson, M. Sandstroem and A.-S. Ullstroem, *J. Chem. Soc., Dalton Trans.*, 2002, 1256-1265.
10. V. J. Burton, R. J. Deeth, C. M. Kemp and P. J. Gilbert, *J. Am. Chem. Soc.*, 1995, **117**, 8407-8415.
11. D. Boldrin and A. S. Wills, *J. Mat. Chem. C*, 2015, **3**, 4308-4315.
12. T. Kubo, A. Hirai and H. Abe, *J. Phys. Soc. Jap.*, 1969, **26**, 1094-1109.
13. A. Avdeef, J. A. Costamagna and J. P. Fackler, Jr., *Inorg. Chem.*, 1974, **13**, 1854-1863.
14. J. P. Fackler, Jr. and A. Avdeef, *Inorg. Chem.*, 1974, **13**, 1864-1875.
15. A. Cornia, A. Caneschi, P. Dapporto, A. C. Fabretti, D. Gatteschi, W. Malavasi, C. Sangregorio and R. Sessoli, *Angew. Chem., Int. Ed.*, 1999, **38**, 1780-1782.
16. P. Wagner, I. Gordon, S. Mangin, V. V. Moshchalkov, Y. Bruynseraede, L. Pinsard and A. Revcolevschi, *Phys. Rev. B: Condens. Matter Mater. Phys.*, 2000, **61**, 529-537.
17. J. Krzystek, G. J. Yeagle, J.-H. Park, R. D. Britt, M. W. Meisel, L.-C. Brunel and J. Telser, *Inorg. Chem.*, 2003, **42**, 4610-4618.
18. J. Goodenough, *Annu. Rev. Mater. Sci.*, 1998, **28**, 1-27.
19. D. J. Price, S. R. Batten, B. Moubaraki and K. S. Murray, *Chem. Commun.*, 2002, 762-763.
20. S. Wang, W.-R. He, M. Ferbinteanu, Y.-H. Li and W. Huang, *Polyhedron*, 2013, **52**, 1199-1205.
21. M. S. Shongwe, M. Mikuriya, E. W. Ainscough and A. M. Brodie, *J. Chem. Soc., Chem. Commun.*, 1994, 887-888.
22. M. A. Halcrow, *Dalton Trans.*, 2003, 4375-4384.
23. V. Uma, M. Kanthimathi, T. Weyhermuller and B. U. Nair, *J. Inorg. Biochem.*, 2005, **99**, 2299-2307.
24. G. Kokoszka, J. Baranowski, C. Goldstein, J. Orsini, A. Mighell, V. Himes and A. Siedle, *J. Am. Chem. Soc.*, 1983, **105**, 5627-5633.
25. J. Ammeter, H. B. Bürgi, E. Gamp, V. Meyer-Sandrin and W. P. Jensen, *Inorg. Chem.*, 1979, **18**, 733-750.
26. M. A. Lafontaine, A. Le Bail and G. Férey, *J. Solid State Chem.*, 1990, **85**, 220-227.
27. H. Effenberger, *Z. Kristall.*, 1989, **188**, 43-56.
28. P. García-Fernández, J. M. García-Lastra, A. Trueba, M. T. Barriuso, J. A. Aramburu and M. Moreno, *Phys. Rev. B*, 2012, **85**, 094110.
29. J. A. Aramburu, J. M. García-Lastra, P. García-Fernández, M. T. Barriuso and M. Moreno, *Inorg. Chem.*, 2013, **52**, 6923-6933.
30. P. G. Sim and E. Sinn, *J. Am. Chem. Soc.*, 1981, **103**, 241-243.
31. G. G. Morgan, K. D. Murnaghan, H. Müller-Bunz, V. McKee and C. J. Harding, *Angew. Chem., Int. Ed.*, 2006, **45**, 7192-7195.
32. Z. L. Liu, S. L. Liang, X. W. Di and J. Zhang, *Inorg. Chem. Commun.*, 2008, **11**, 783-786.
33. B. Gildea, L. C. Gavin, C. A. Murray, H. Müller-Bunz, C. J. Harding and G. G. Morgan, *Supramol. Chem.*, 2012, **24**, 641-653.
34. P. N. Martinho, B. Gildea, M. M. Harris, T. Lemma, A. D. Naik, H. Müller-Bunz, T. E. Keyes, Y. Garcia and G. G. Morgan, *Angew. Chem. Int. Ed.*, 2012, **50**, 12597–12601
35. K. Pandurangan, B. Gildea, C. Murray, C. J. Harding, H. Müller-Bunz and G. G. Morgan, *Chem. Eur. J.*, 2012, **18**, 2021-2029.
36. B. Gildea, M. M. Harris, L. C. Gavin, C. A. Murray, Y. Ortin, H. Müller-Bunz, C. J. Harding, Y. Lan, A. K. Powell and G. G. Morgan, *Inorg. Chem.*, 2014, **53**, 6022-6033.
37. M. S. Shongwe, K. S. Al-Barhi, M. Mikuriya, H. Adams, M. J. Morris, E. Bill and K. C. Molloy, *Chem. Eur. J.*, 2014, **20**, 9693-9701.

38. J. Sirirak, D. J. Harding, P. Harding, K. S. Murray, B. Moubaraki, L. Liu and S. G. Telfer, *Eur. J. Inorg. Chem.*, 2015, n/a-n/a.
39. S. Wang, Y.-H. Li and W. Huang, *Eur. J. Inorg. Chem.*, 2015, **2015**, 2237-2244.
40. S. I. Klokishner, M. A. Roman and O. S. Reu, *Inorg. Chem.*, 2011, **50**, 11394-11402.
41. S. Wang, M. Ferbinteanu, C. Marinescu, A. Dobrinescu, Q. D. Ling and W. Huang, *Inorg. Chem.*, 2010, **49**, 9839-9851.
42. Y. Sawada, S. Kimura, K. Watanabe and M. Nakano, *J. Low Temp. Phys.*, 2013, **170**, 424-429.
43. S. Kimura, T. Otani, Y. Narumi, K. Kindo, M. Nakano and G.-e. Matsubayashi, *J. Phys. Soc. Jpn.*, 2003, **72**, 122-126.
44. M. Nakano, G. Matsubayashi and T. Matsuo, *Phys. Rev. B*, 2002, **66**.
45. Y. Garcia, O. Kahn, J.-P. Ader, A. Buzdin, Y. Meurdesoif and M. Guillot, *Phys. Lett. A*, 2000, **271**, 145-154.
46. P. Guionneau, M. Marchivie, Y. Garcia, J. A. Howard and D. Chasseau, *Phys. Rev. B*, 2005, **72**, 214408.
47. M. Nakano, G.-e. Matsubayashi and T. Matsuo, in *Adv. Quantum Chem.*, 2003, **44**, 617-630.
48. Y. Garcia, H. Paulsen, V. Schunemann, A. X. Trautwein and J. A. Wolny, *PCCP*, 2007, **9**, 1194-1201.
49. M. A. Halcrow, *Coord. Chem. Rev.*, 2009, **253**, 2493-2514.
50. R. Pritchard, S. A. Barrett, C. A. Kilner and M. A. Halcrow, *Dalton Trans.*, 2008, 3159-3168.
51. N. Nagels, D. Hauchecorne and W. Herrebout, *Molecules*, 2013, **18**, 6829.
52. A. K. Jordao, V. F. Ferreira, A. C. Cunha, J. L. Wardell, S. M. S. V. Wardell and E. R. T. Tiekink, *CrystEngComm*, 2012, **14**, 6534-6539.
53. Y.-X. Lu, J.-W. Zou, Y.-H. Wang and Q.-S. Yu, *Int. J. Quantum Chem*, 2007, **107**, 1479-1486.
54. I. Bersuker, *The Jahn-Teller Effect*, Cambridge University Press, 2006.